Available online at www.sciencedirect.com

ScienceDirect

Catalysis Today 117 (2006) 32–36

CATALYSIS TODAY

www.elsevier.com/locate/cattod

Molecular design of selective oxidation catalyst with polyoxometalate

Noritaka Mizuno [a,b,*], Shiro Hikichi [a,b], Kazuya Yamaguchi [a,b], Sayaka Uchida [a,b],
Yoshinao Nakagawa [a], Kazuhiro Uehara [b], Keigo Kamata [b]

[a] *Department of Applied Chemistry, School of Engineering, The University of Tokyo,*
7-3-1 Hongo, Bunkyo-ku, Tokyo 113-8656, Japan
[b] *Core Research for Evolutional Science and Technology (CREST), Japan Science and Technology Agency,*
4-1-8 Honcho, Kawaguchi, Saitama 332-0012, Japan

Abstract

Efficient H_2O_2-based oxidation systems with three kinds of polyoxometalates, $[\gamma\text{-SiW}_{10}O_{34}(H_2O)_2]^{4-}$ (**1**), $[\gamma\text{-1,2-H}_2\text{SiV}_2\text{W}_{10}O_{40}]^{4-}$ (**2**), and $[W_2O_3(O_2)_4(H_2O)_2]^{2-}$ (**3**) are reported. The compound **1** can catalyze epoxidation of various olefins including non-activated terminal olefins such as propylene and 1-octene with $\geq$99% selectivity to epoxide and $\geq$99% efficiency of H_2O_2 utilization. It is notable that **2** shows unique stereospecificity, regioselectivity, and diastereoselectivity for the epoxidation of *cis*/*trans* olefins, non-conjugated dienes, and 3-substituted cyclohexenes, respectively. The epoxidation of various allylic alcohols with only 1 equiv. H_2O_2 in water can be efficiently catalyzed by **3** to give the corresponding epoxy alcohols in high yields. Further, the catalyst **3** can be recycled with the maintenance of the catalytic performance.
© 2006 Elsevier B.V. All rights reserved.

Keywords: Allylic alcohols; Hydrogen peroxide; Olefins; Oxidation; Polyoxometalates

1. Introduction

In the preceding few decades, the use of polyoxometalates (POMs) and POM-based compounds as catalysts has become a very important research area. Especially, POMs have received much attention in the area of acid and oxidation catalysis because their acidic and redox properties can be controlled at the molecular or atomic level [1–8]. The additional attractive and technologically significant aspect of POMs in catalysis is that they are thermally and oxidatively stable compared with organometallic complexes [1–8]. Various types of POMs have been synthesized by the proper selection of the starting components and by the adjustment of pH and temperature, and can act as effective catalysts for oxidations with environmentally friendly O_2 or H_2O_2 [1–8].

A wide variety of hydrocarbons including alkanes, alcohols, amines, and arenes can be oxidized with O_2 in the presence of mixed-addenda POMs $[PMo_{12-n}V_nO_{40}]^{(3+n)-}$ [9–17]. The mechanism included one electron oxidation of the substrate by $[PMo_{12-n}V_nO_{40}]^{(3+n)-}$ to form the product and the reduced $[PMo_{12-n}V_nO_{40}]^{(4+n)-}$, followed by reoxidation of the reduced catalyst by O_2. In 1986, it was reported for the first time by Hill and Brown that transition-metal-substituted POMs $[PW_{11}O_{39}M'(OH_2)]^{5-}$ ($M' = Mn^{2+}$, Co^{2+}) catalyzed the oxidation of olefins with PhIO [18]. The active sites of transition-metal-substituted POMs can be controlled at the molecular or atomic level. These advantages have been applied to the development of bio-inspired inorganic catalysts relating to the analogues of the heme enzyme, cytochrome P-450, and the non-heme enzymes including methane monooxygenase. Until now, numerous transition-metal-substituted POMs have been reported for catalytic selective oxidations [18–27] and $[WZnRu_2(OH)(H_2O)(XW_9O_{34})_2]^{11-}$ [19], $[\gamma\text{-SiW}_{10}\{Fe(OH_2)\}_2O_{38}]^{6-}$ [21], and $[(CH_3CN)_xFe\cdot SiW_9V_3O_{40}]^{5-}$ [22] are examples active for oxidation with O_2.

Tungsten-based POMs and the related compounds show high efficiency of H_2O_2 utilization [28–40]. Ishii et al. have developed effective H_2O_2-based epoxidation of olefins catalyzed by $H_3PW_{12}O_{40}$ combined with cetyl pyridinium chloride as a phase transfer agent [29]. The $[PO_4\{WO(O_2)_2\}_4]^{3-}$ peroxotungstate was isolated and crystallographically characterized by Venturello and co-workers [30,31]. This peroxo anion has been postulated to be catalytically the most active species in the $H_3PW_{12}O_{40}/H_2O_2$ system because $[PO_4\{WO(O_2)_2\}_4]^{3-}$ exhib-

---

* Corresponding author. Tel.: +81 3 5841 7272; fax: +81 3 5841 7220.
E-mail address: tmizuno@mail.ecc.u-tokyo.ac.jp (N. Mizuno).

0920-5861/$ – see front matter © 2006 Elsevier B.V. All rights reserved.
doi:10.1016/j.cattod.2006.05.002

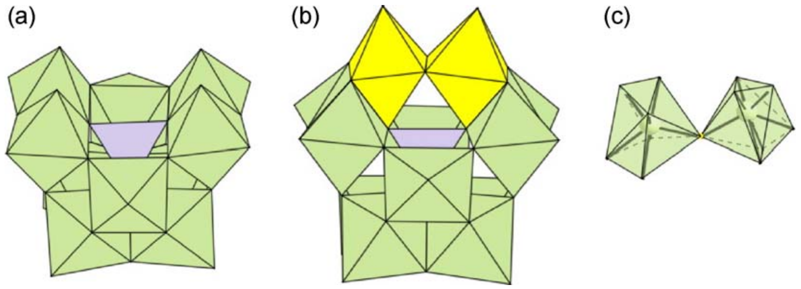

Fig. 1. Polyhedral representations of: (a) $[\gamma\text{-SiW}_{10}O_{34}(H_2O)_2]^{4-}$, (b) $[\gamma\text{-1,2-H}_2\text{SiV}_2W_{10}O_{40}]^{4-}$, and (c) $[W_2O_3(O_2)_4(H_2O)_2]^{2-}$. The WO_6 moieties occupy the green octahedra, and SiO_4 groups are shown as internal gray tetrahedra. In the case of $[\gamma\text{-1,2-H}_2\text{SiV}_2W_{10}O_{40}]^{4-}$, the two vanadium atoms are represented by yellow octahedra.

ited catalytic reactivity similar to that of Ishii-system [32,33]. Recently, Noyori and co-workers reported an H_2O_2-based oxidation system of tungstate and methyltrioctylammonium hydrogensulfate without halides and organic solvents [38–40].

In this paper, we report efficient H_2O_2-based oxidation systems based on three kinds of POMs, a divacant lacunary polyoxotungstate $[\gamma\text{-SiW}_{10}O_{34}(H_2O)_2]^{4-}$ (**1**, Fig. 1a) [34,35], a di-vanadium-substituted polyoxotungstate $[\gamma\text{-1,2-H}_2\text{SiV}_2W_{10}O_{40}]^{4-}$ (**2**, Fig. 1b) [41], and a dinuclear peroxotungstate $[W_2O_3(O_2)_4(H_2O)_2]^{2-}$ (**3**, Fig. 1c) [36,37].

2. Experimental

2.1. Synthesis of tetra-n-butylammonium salt of $[\gamma\text{-SiW}_{10}O_{34}(H_2O)_2]^{4-}$ (TBA-**1**)

$K_8[\gamma\text{-SiW}_{10}O_{36}]\cdot 12H_2O$ [42] (6 g, 2 mmol) was dissolved in 60 mL of water, and the pH of this aqueous solution was carefully adjusted to 2 with HNO_3. After stirring the solution for 15 min at room temperature, an excess amount of $[(n\text{-}C_4H_9)_4N]Br$ (6.46 g, 20 mmol) was added in a single step. The resulting white precipitate of TBA-**1** was collected by the filtration and then washed with an excess amount of water. After the dryness, the crude product was purified twice with the precipitation method. Analytically pure TBA-**1** was obtained as a white powder. Yield 3.4 g (54%). Anal. calcd. for $[(n\text{-}C_4H_9)_4N]_4[\gamma\text{-SiW}_{10}O_{34}(H_2O)_2]\cdot H_2O$: C, 22.09; H, 4.19; N, 1.64; Si, 0.80; W, 53.24. Found: C, 22.38; H, 4.40; N, 1.63; Si, 0.82; W, 53.53. ^{29}Si NMR (CD_3CN/DMSO (2/1 v/v), 53.45 MHz): −83.5 ppm. ^{183}W NMR (CD_3CN/DMSO (2/1 v/v), 11.20 MHz): −95.7, −98.9, −118.2, −119.6, −195.7 ppm with the integrated intensity ratio of 1:1:1:1:1, respectively. UV–vis (CH_3CN): 275 nm ($\varepsilon = 22{,}000\ M^{-1}\ cm^{-1}$). IR (KBr) ($cm^{-1}$): 999, 958, 920, 902, 877, 784, 745, 691, 565, 544.

2.2. Synthesis of tetra-n-butylammonium salt of $[\gamma\text{-1,2-H}_2\text{SiV}_2W_{10}O_{40}]^{4-}$ (TBA-**2**)

Aqueous solution of $[\gamma\text{-1,2-H}_2\text{SiV}_2W_{10}O_{40}]^{4-}$ was prepared according to Ref. [43], and the anion was isolated as the tetra-*n*-butylammonium salt. $K_8[\gamma\text{-SiW}_{10}O_{36}]\cdot 12H_2O$ [42] (8 g, 2.7 mmol) was quickly dissolved in 1 M HCl (28 mL). $NaVO_3$ (0.5 M, 11 mL, 5.5 mmol) was added, and the mixture was gently stirred for 5 min. The solution was filtered off followed by the addition of $[(n\text{-}C_4H_9)_4N]Br$ (8 g, 25 mmol) in a single step. The resulting yellow precipitate was collected by the filtration and then washed with an excess amount of water (300 mL). The crude product was purified twice with the precipitation method. Analytically pure TBA-**2** was obtained as a pale yellow powder. Yield: 7.43 g (76%). Anal. calcd. for $[(C_4H_9)_4N]_4[\gamma\text{-1,2-H}_2\text{SiV}_2W_{10}O_{40}]\cdot H_2O$: C, 21.4; H, 4.15; N, 1.56; Si, 0.78; V, 2.83; W, 51.1. Found: C, 21.4; H, 3.91; N, 1.59; Si, 0.79; V, 2.88; W, 51.2. ^{51}V NMR (CD_3CN, 70.90 MHz): −563.6 ppm. ^{29}Si NMR (CD_3CN, 53.45 MHz): −84.0 ppm. ^{183}W NMR (CD_3CN, 11.20 MHz): −82.2, −95.6, −129.7 ppm with an integrated intensity ratio of 2:1:2, respectively. UV–vis (CH_3CN) 240 ($\varepsilon = 36{,}000\ M^{-1}\ cm^{-1}$), 285 ($\varepsilon = 24{,}000\ M^{-1}\ cm^{-1}$), 350 nm ($\varepsilon = 5900\ M^{-1}\ cm^{-1}$). IR (KBr) ($cm^{-1}$): 1151, 1106, 1057, 1004, 995, 966, 915, 904, 875, 840, 790, 691, 550, 519, 482, 457, 405.

2.3. Synthesis of potassium salt of $[W_2O_3(O_2)_4(H_2O)_2]^{2-}$ (K-**3**)

The compound K-**3** was synthesized according to the procedure in Ref. [44]. Anal. calcd. for $K_2[W_2O_3(O_2)_4(H_2O)_2]\cdot 2H_2O$: H, 1.16; K, 11.27; W, 52.99. Found: H, 1.12; K, 11.98; W, 53.19. ^{183}W NMR (D_2O, 11.2 MHz): −704.5 ppm. UV–vis (H_2O): 243 nm ($\varepsilon = 608\ M^{-1}\ cm^{-1}$). IR (KBr) ($cm^{-1}$): 966, 854, 764, 615, 566, 332.

2.4. Catalytic oxidation

The epoxidation of gaseous substrates (propylene and 1-butene) was carried out with a Teflon coated autoclave. For the other substrates, a glass tube reactor was used. Detailed reaction conditions were given in the footnotes of tables. The reaction solution was periodically sampled and analyzed by GC or ^{1}H NMR. The products were identified by the comparison of mass and NMR spectra with those of authentic samples. Remaining H_2O_2 after the reaction was analyzed by the $Ce^{4+/3+}$ titration [45].

3. Results and discussion

3.1. Epoxidation of olefins catalyzed by $[\gamma\text{-SiW}_{10}O_{34}(H_2O)_2]^{4-}$

The epoxidation of 1-octene with a series of silicotungstates and peroxotungstates in acetonitrile at 305 K was examined